Agriculture, Ecosystems and Environment 399 (2026) 110146

Contents lists available at ScienceDirect

Agriculture, Ecosystems and Environment

journal homepage: www.elsevier.com/locate/agee

Mitigating greenhouse gas emissions of a managed organic soil by paddy rice cultivation in the cool temperate zone

Alina Widmer [a,d,*], Lisa Tamagni [b,c], Chloé Wüst-Galley [b], Sonja Paul [b], Markus Jocher [b], Valerio Volpe [a], Sebastian Doetterl [d], Thomas Keller [a,e], Jens Leifeld [b]

[a] Soil Quality and Soil Use Group, Agroscope, Reckenholzstrasse 191, Zurich 8046, Switzerland
[b] Climate and Agriculture Group, Agroscope, Reckenholzstrasse 191, Zurich 8046, Switzerland
[c] Department of Geography, University of Zurich, Winterthurerstrasse 190, Zurich 8057, Switzerland
[d] Department of Environmental System Science, ETH Zurich, Rämistrasse 101, Zurich 8092, Switzerland
[e] Department of Soil and Environment, Swedish University of Agricultural Sciences, Almas Allé 8, Uppsala 750 07, Sweden

ARTICLE INFO

Keywords:
CO_2
CH_4
N_2O
Mineral cover
Rewetting
Paludiculture
Peatland

ABSTRACT

Large areas of temperate peatlands are drained for agriculture and are strong sources of greenhouse gases (GHG). Paddy rice cultivation as a new cropping system in the cool temperate climate could offer an opportunity for continuing food production on these organic soils, possibly reducing carbon dioxide (CO_2) and nitrous oxide (N_2O) emissions by rewetting. However, methane (CH_4) from paddy rice cultivation might impair the potential climate benefits. Here, the GHG fluxes of CO_2, CH_4, and N_2O of paddy rice grown on organic soil with and without amended mineral cover, as well as in ley cultivated on drained organic soil as a reference, were quantified in an outdoor mesocosm experiment in Switzerland (cool temperate climate). Measurements were conducted with manual chambers for one year. Compared to ley under drained management, paddy rice cultivation reduced the net GHG balance by 36.1 %, from 32.7 (7.0) to 20.9 (2.7) t CO_2 eq ha^{-1} yr^{-1}. The GHG balance was dominated by CO_2 whereas CH_4 accounted for 8 % (54.3 (26.2) kg CH_4 ha^{-1} yr^{-1}). Most CO_2 emissions occurred during the drained fallow period (mid-September–April). N_2O emissions (0.9 (0.4) kg N_2O-N ha^{-1} yr^{-1}) were reduced by 83.9 % with paddy rice. Adding an amended mineral cover to organic soil slightly reduced the net GHG balance further, but not significantly. Multi-year studies on field-scale are required to generalize this study's findings derived from a one-year mesocosm experiment. The results point towards paddy rice cultivation being a promising alternative to drained agriculture on temperate organic soils while maintaining food production and mitigating GHG emissions.

1. Introduction

In their natural wet state, peatlands form organic soils, which are among the largest terrestrial carbon reservoirs, estimated to be between 500 and 600 Pg C (Leifeld and Menichetti, 2018; United Nations Environment Programme (UNEP) (UNEP).,2022). However, large-scale drainage for agriculture and forestry has turned many organic soils from a carbon sink into a carbon source, mostly owing to microbial peat oxidation, resulting in accumulated emissions of 80 (20) Pg CO_2-eq. globally or approximately 1.9 Pg CO_2-eq. per year (Leifeld et al., 2019). This problem is most accentuated in Europe, where 46 % of peatlands are degraded and emit currently 582 Mt CO_2-eq. per year (Tanneberger et al., 2021b; United Nations Environment Programme (UNEP) (UNEP)., 2022). Alongside GHG emissions, managed temperate peatlands in Europe are affected by soil subsidence, which poses risks to the sustained use of these soils for agriculture (Erkens et al., 2016; Leifeld et al., 2011; Tanneberger et al., 2021a).

It is widely acknowledged that water level is the primary control of organic soil decomposition in peatlands (Evans et al., 2021; Freeman et al., 2022; Koch et al., 2023; Tiemeyer et al., 2020). Raising the water table of drained organic soils is therefore the most effective known measure to strongly reduce CO_2 emissions (Freeman et al., 2022; Tanneberger et al., 2021b). Introducing flooded conditions can strongly reduce the oxygen supply necessary for aerobic organic matter decomposition. Agriculturally managed peatlands can either be rewetted by abandonment of agriculture or by switching to paludiculture (Bianchi

* Corresponding author at: Soil Quality and Soil Use Group, Agroscope, Reckenholzstrasse 191, Zurich 8046, Switzerland
E-mail address: alina.widmer@agroscope.admin.ch (A. Widmer).

https://doi.org/10.1016/j.agee.2025.110146
Received 6 August 2025; Received in revised form 26 November 2025; Accepted 29 November 2025
Available online 4 December 2025

et al., 2021). Paludiculture is a form of agriculture whereby plants tolerant of waterlogged conditions, such as *Sphagnum* or *Typha*, are cultivated under high-water tables (Joosten et al., 2015), mostly to produce bioenergy or fiber. Paludiculture reduces CO_2 emissions and soil degradation efficiently (Bianchi et al., 2021; Tanneberger et al., 2022), but only 1 % of degraded peatlands are currently rewetted in Europe (United Nations Environment Programme (UNEP) (UNEP)., 2022). One reason for this is the economic challenges associated with paludicultures in comparison to current drained peatland use (Buschmann et al., 2020; Ferré et al., 2019; Rawlins and Morris, 2010). Reduced food security remains an additional limitation, either because most crops currently grown in cool temperate paludiculture are not edible (Tanneberger et al., 2021b) or because agriculture with raised water tables is associated with reduced biomass production (Freeman et al., 2022).

A potential solution for organic soil management that can address the combined challenges of mitigating climate change while maintaining food security could be the cultivation of rice, the world's most significant water-tolerant staple crop. With the accompanying high water table, CO_2 and N_2O emissions are predicted to decline strongly. However, paddy rice cultivation is notorious for its high methane (CH_4) emissions under anaerobic conditions and, globally, accounts for 8 % of anthropogenic CH_4 emissions (Saunois et al., 2024). Indeed, compared to wheat and maize, two other globally important staple crops, the yield-scaled GHG emissions of paddy rice on mineral soil is four times higher, mainly due to CH_4 emissions (Linquist et al., 2012). The much higher GHG emissions of rice cited above relates to cultivation on mineral soils. Relative to upland crop cultivation on drained organic soils, however, paddy rice cultivation on organic soil could have a lower GHG balance, due to the reduced CO_2 and N_2O emissions. In Europe, paddy rice is grown successfully on mineral soil under a warm temperate climate in Italy, Spain, and Southern France (Kraehmer et al., 2017). Traditionally, rice could not be cultivated under the cool temperate climate of Northern and Central Europe; however, changing climate conditions under global warming are shifting possible rice cropping regions. It is predicted that within the next four decades, the area suitable for rice cropping would touch high latitudes up to 60° north, thereby including large parts of currently drained European peatland areas (Su et al., 2021). Indeed, paddy rice cultivation was successfully introduced for the first time north of the Alps in Switzerland in 2017 (Fabian et al., 2022). Today, farmers sell rice directly as an economically viable local niche product (Fabian et al., 2024). Given this recent development, the GHG balance of paddy rice cultivation in the temperate climate outside of the Mediterranean region, and therefore the possible implications for organic soil management, is unknown.

This study compares the full GHG balance (i.e., CO_2, CH_4, N_2O, and harvest export) of paddy rice cultivation on organic soil under cool temperate climate with that of typical management of these soils for agriculture—that is, drained ley—in an outdoor mesocosm experiment. The authors hypothesize that paddy rice cultivation improves the overall GHG balance by reduced CO_2 and N_2O emissions in spite of higher CH_4 emissions. Additionally, this study tests whether the GHG balance of paddy rice cultivation on organic soil can be further improved by applying a mineral soil cover on top of the organic soil, which has previously shown positive effects on CH_4 and N_2O emissions (Paul et al., 2024; Wang et al., 2022; Wüst-Galley et al., 2023). This paper provides novel insights as the full GHG balance including all major GHGs (CO_2, CH_4, N_2O) of paddy rice cultivation on organic soils has never been measured before in the temperate cool climate. Furthermore, this study provides evidence on the effect of a mineral soil cover on organic soil on the full GHG balance and suggests rice as a new and edible paludiculture crop for the cool temperate zone of Europe.

2. Materials and methods

2.1. Experimental setup

2.1.1. Site description

The outdoor mesocosm facility is located at the Agroscope research institute in Zurich (47.42796° N, 8.51769° E), at 444 m above sea level in the Swiss plateau. The climate zone is cool temperate according to the IPCC classification (Bickel et al., 2006), with a mean annual temperature of 9.8°C and a mean annual precipitation of 1022 mm. The outdoor mesocosm experiment was composed of eight rows with six concrete-lined mesocosms per row and the option to actively control or fluctuate the water table of each row with an automatic system during the runtime of the experiment. Each mesocosm was 1.2 m long, 1.2 m wide, and 1.4 m deep. To increase the water level, the system pumped water into an inspection well located at the end of each row. The water then moved through a pipe that ran along the bottom of the row and into each of the six mesocosms. The six mesocosms were thus connected hydraulically, but a metal grate at the base of each mesocosm ensured that the plots were otherwise disconnected. To actively remove water from the mesocosms, water was pumped out of the inspection well (Figure S1). To ensure independence despite hydraulic connection, all replicates per treatment ($n = 4$) were located in different rows except for the drained mesocosms where the effect of the hydraulic connection was assumed to be negligible. The mesocosms were divided in half in the middle by a 0.05-m-thick concrete slab to a depth of 0.3 m. In one half, gas measurements were taken, while in the other half, soil temperature, soil moisture, and redox potential were measured. The two sides of each plot were managed identically.

2.1.2. Experimental treatments

Three treatments were compared. Mesocosms filled with organic soil and cultivated as paddy rice under flooded conditions were labeled 'flooded rice' (FR). The second paddy rice treatment had an amended mineral cover over organic soil and was also in flooded conditions denoted as 'flooded rice with amended mineral cover' (FR+AC). As a well-aerated reference treatment, ley (*Lolium perenne*) was grown on organic soil under drained conditions named 'drained ley' (DL).

2.1.3. Soil properties

In March 2020, all mesocosms were filled with organic soil classified as degraded fen peat taken from a nearby site that had been drained and managed for agriculture for several decades. Soils with a soil organic carbon (SOC) content > 20 % are classified as organic soils while soils below this threshold are considered mineral soils (IUSS Working Group., 2022). The organic soil had a pH of 6.0, 27.4 % SOC content, and a C/N ratio of 20. The mesocosm used for the amended mineral cover/organic soil combination was filled with organic soil to a depth of only 0.3 m below the surface. The remaining 0.3 m was filled with a mineral soil cover. This mineral soil was classified as a loam (12 % clay, 46 % silt, 42 % sand), with a pH of 7.6, SOC content of 0.6 % and C/N ratio of 12.6 (Wüst-Galley et al., 2023). After adding the mineral soil, compost derived from tree- and bush cuts (10 kg dry mass per plot, pH 8.1, organic carbon content 20.5 %, C/N-ratio 13.2) was mixed into the mesocosm in 2020 to increase its biological activity, as is common in agricultural practice. Similarly, mineral soil is used by farmers to cover organic soils under agricultural use in Switzerland (Paul et al., 2024). Since compost and mineral soil were mixed for the amended mineral cover this study cannot account for the effect of compost addition by itself nor the effect of mineral soil alone.

2.1.4. Water management

While the rice mesocosms were flooded during the growing season, the water table was kept, on average, at + 0.045 (0.012) m above the soil surface (Figure S2). Flooding began on 11 April 2023 and lasted for 28 days, until the mesocosms were drained for seedling transplantation.

The mesocosms were then flooded again for 33 days until they were drained for several hours to apply fertilizer, a procedure repeated 36 days later. Mid-season drainage started on 7 August 2023, with the mesocosms completely drained for 9 days. Thereafter, the rice mesocosms were flooded again for 17 days until drainage for harvest on 11 September 2023. After harvest and during winter, the rice mesocosms remained drained until they were flooded again in spring.

For the DL mesocosms, the water table was, on average, −1.0 (0.06) m throughout the season (Figure S2). In the absence of rain, the DL mesocosms were irrigated during the growing season. Due to hot and dry conditions in June, the water table in the DL mesocosms was raised for a day to eliminate drought-related crevasses between the peat and the mesocosm walls and to ensure representative ley growth (Figure S2).

2.1.5. Cultivation

Eight mesocosms were planted with rice variety *Loto* (*Oryza sativa* L.). Rice seeds were sown in a potting substrate and cultivated in a greenhouse for one month. During this time, seedlings were fertilized twice with Wuxal® (Syngenta), an NPK mineral fertilizer with additional micronutrients (K, B, Cu, Fe, Mn, Mo, Zn). On 17 May 2023, 34 seedlings were transplanted to each rice mesocosm. Rice mesosoms were fertilized on 9 May, 19 June, and 25 July 2023 with Wuxal® (Syngenta) and an additional NPK mineral fertilizer, receiving a total of 110 kg N ha^{-1} yr^{-1} according to national fertilization recommendations (Huguenin-Elie et al., 2017). On each fertilization date, one third of the total N amount was applied (36.7 kg N ha^{-1}). At harvest (19 September 2023), the panicles and straw were removed from the mesocosms. Subsequently, the rice straw was dried, shredded, and incorporated into the mesocosms in November 2023. In the previous year, rice straw was removed from the mesocosms. Panicles, representing a loss of carbon (C_{export}), were not returned to the plots since this is not common practice. The carbon content of the rice grains was obtained by dry combustion (DIN,2022). The unpolished rice yield was 4.8 (0.5) t/ha in FR and 4.3 (0.8) t/ha in FR+AC and did not differ significantly ($p = 0.94$).

Four mesocosms were planted with ley (*Lolium perenne L*). The ley was cut twice (14 July and 3 October 2023), and the harvested biomass was exported. The exported ley biomass was dried and weighed, and 45 % carbon content of ley was derived from literature values (Bolinder et al., 2012; Ma Su Hui et al.,2018) to obtain C_{export}. The ley was fertilized according to national fertilizer recommendations (Huguenin-Elie et al., 2017) on 9 May, 19 June, and 25 July 2023 with Wuxal® (Syngenta) and an additional NPK mineral fertilizer, receiving a total of 38 kg N/yr^{-1} ha^{-1}. On each fertilization date, one third of the total N amount was applied in the ley mesocosms (12.7 kg N ha^{-1}).

2.1.6. Soil sensors

Soil temperature and soil water content of each plot were measured at a depth of 0.05 m using Teros-11 soil sensors (METER Group), recording data at an interval of 15 min (Figure S3 and S4). Redox conditions were monitored using self-developed probes (Reiser et al., 2020) placed 0.05 m deep, with two probes installed per mesocosm. These probes recorded redox potential every 8 h during the rice growing season from 17 May to 19 September 2023 (Figure S5).

2.2. Gas flux measurements

Measurements were conducted using two different manual chambers with dimensions of 1.2 m length, 0.605 m width, and 0.795 m height, resulting in a total volume of 0.57 m^3 . Both chambers were equipped with two fans to ensure gas circulation. Gas measurements took place from 1 May 2023–30 April 2024.

2.2.1. CO_2 measurements

CO_2 fluxes were measured with a transparent chamber. CO_2 concentration was measured with an infrared CO_2 probe (GMP343 diffusion model, Vaisala, Vantaa, Finland). A separate probe (Vaisala, Vantaa, Finland) was connected to a logger (MI70 Indicator, Vaisala), and relative humidity and temperature were measured from within the chamber. During the rice growing season (17 May–19 September 2023), measurements were conducted at a weekly interval with a higher frequency around drainage events (mid-season drainage and harvest drainage). Off-season (19 September 2023–30 April 2024), the frequency was reduced to a biweekly interval or longer if weather conditions were unsuitable. On a measurement day, net ecosystem exchange (NEE) measurements were taken with a resolution of 5 s for 2 min at a time between 2 h before and after solar noon under a bright, cloudless sky with full sunlight and maximum solar radiation. This was done to ensure that the maximum gross primary production (GPP_{max}) could be calculated from the CO_2 measurements. Light response curves were generated (two for DL and one for FR and FR+AC) by measuring from 1 h before sunrise to 1 h after sunset, on cloudless days. Ecosystem respiration (R_{eco}) measurements were carried out on the same day as the NEE measurements and took place 1 h after sunset, and each measurement lasted for 5 min. Minimal detectable flux as calculated according to Maier et al. (2022) was 0.028 g CO_2 m^{-2} h^{-1}.

2.2.2. CH_4 and N_2O measurements

An opaque chamber was used for the CH_4 and N_2O measurements. The gases were measured with a Picarro G2308 gas analyzer with a resolution of one second (Picarro Inc., USA). The chamber air temperature was measured during each gas measurement using a thermometer mounted within the chamber. During the rice season, measurements were conducted twice a week, or more frequently if a significant change in the water table was manually introduced or if fertilizer was applied. Off-season measurements took place monthly. In April 2024, no CH_4 and N_2O measurements were performed in the DL mesocosms. The chamber was placed on each mesocosm for 15 min for each measurement. Gas concentration curves were checked visually for irregularities that indicated leakage of the system. Additionally, for this error assessment, the first 3 min of data were omitted from each measurement to remove any irregularities caused by the lowering of the chamber, resulting in 12 min measurements. Minimal detectable flux as calculated according to Maier et al. (2022) was 0.0014 mg CH_4 m^{-2} h^{-1} and 0.075 mg N_2O-N m^{-2} h^{-1}.

2.3. Flux calculations and GHG balance

2.3.1. CO2 fluxes

To account for gas pressure equilibration, the first 20 s of each CO_2 measurement were discarded. A linear regression was fitted through the remaining 20 measurement points. Measurements were only included for calculation if they had a $R^2 > 0.75$. Measurements with no clear increase or decrease in CO_2 concentration were accepted if the change in CO_2 concentrations was smaller than 3 % of the mean CO_2 concentration (Oestmann et al.,2022). Lastly, 20 % of the NEE measurements were discarded because the air temperature in the chamber increased > 3°C during the measurement, which results in an overestimation of CO_2 uptake (Drösler, 2005). Due to variations in the water table between flooded and drained periods and between mesocosms, the volume of air within the chamber was adjusted for flux determination. The volume of plants grown in the mesocosms was estimated and considered negligible (Lim et al., 2021).

To assess the overall carbon balance, the system's NEE was calculated on a continuous basis. As CO_2 fluxes were measured discontinuously, the widely used approach of parameterizing the two underlying fluxes of NEE with opposite signs, namely plant uptake (i.e., gross primary production GPP) and ecosystem respiration (R_{eco}) was applied as follows:

$$NEE = GPP + R_{eco} \quad (1)$$

R_{eco} can be obtained in the absence of sunlight during the night, when it equals NEE. To obtain R_{eco} for daytime, a R_{eco} model was fitted to the measured R_{eco} values of the night and applied to daytime

temperatures (Lloyd and Taylor, 1994; Richardson et al., 2006) using:

$$R_{eco} = R_{10} + \exp\left[E_0\left(\frac{1}{T_{Ref} - T_0} - \frac{1}{T - T_0}\right)\right] \quad (2)$$

R_{eco} is a function of soil temperature and is described in the Arrhenius function, where R_{10} is the respiration at a reference temperature of 10°C, E_0 represents the long-term ecosystem sensitivity coefficient, T_{Ref} stands for the given reference temperature (10°C), T is the soil temperature measured at 0.05 m depth, and T_0 is the activation temperature 46.02°C (Jurasinski et al., 2014).

For all the following carbon flux calculations,the R package *flux* was used (Jurasinski et al. (2014). Since R_{eco} strongly differs between flooded and drained conditions, two fits for each of these conditions were performed using Eq. 2. Since R_{eco} measurements could not be conducted during the warmest time of the day due to photosynthesis interference, extrapolation of R_{eco} beyond the temperature range with existing R_{eco} measurements was necessary. The maximum temperature for which R_{eco} measurements were available denoted the extrapolation threshold for each treatment. Beyond the extrapolation threshold, all R_{eco} measurements of one treatment were pooled to calculate one model per treatment to reduce the impact of outlier mesocosms. Below the extrapolation threshold, each mesocosm was modeled separately with its corresponding measurements. Extrapolation accounted for 12.5 (4.1) % of total annual R_{eco} in FR, 24.2 (9.0) % in FR+AC, and 14.9 (1.9) % in DL. If the extrapolated part is omitted from total R_{eco}, the difference between FR and DL remains significant. Therefore, the beneficial effect of flooding on R_{eco} remains clear, despite extrapolation.

The resulting R_{eco} models were then used for parametrization in combination with the continuous soil temperature measurements to obtain continuous R_{eco} values throughout the measurement period. R_{eco} models were also used to simulate the effect of off-season flooding on R_{eco} by considering the flooded R_{eco} models instead of the drained ones for the time interval mid-September 2023 to April 2024.

To obtain the GPP outside of the solar noon for the calculation of continuous CO_2 uptake, global radiation (GR) measurements and a light-response curve are necessary. The light-response curve shows the relationship between global radiation and the resulting GPP and is described in the Michaelis–Menten model (Johnson and Goody, 2011). The equation used to calculate continuous GPP is as follows (Volk et al., 2011):

$$GPP = \frac{GPP_{max} \bullet \alpha \bullet GR}{\alpha \bullet GR + GPP_{max}} \quad (3)$$

α denotes the ecosystem quantum yield and represents the starting slope of the light-response curve. To obtain α, a whole-day measurement campaign was conducted starting 1 h before sunrise and ending 1 h after sunset, covering a whole diurnal and cloudless GPP cycle. A nearby (~50 m distance to experimental sites) meteorological station measured GR at a 10-min interval. To obtain GPP throughout the measurement period, the gaps between each GPP_{max} measurement (see Section 2.2.1) were filled by linear interpolation, which enabled continuous calculation of GPP in a 10-min interval, according to Eq. 3. After ley and rice harvest, GPP_{max} was set to zero until the next measurement, which took place 9 days later. The annual CO_2 uptake was then calculated by summing all calculated GPP values. Annual GPP of the rice plants and ley were cross validated by comparing them to the total biomass C by taking root-shoot ratio from Sriskandarajah et al. (2024) and C loss as root exudates (Liu et al., 2019) for rice and root-shoot ratio for ley (Crush et al., 2009). For details see Supplementary Information (Table S1).

2.3.2. CH_4 and N_2O fluxes

Flux calculations for CH_4 and N_2O were performed according to Wüst-Galley et al. (2023). Gas fluxes were determined using the "gasfluxes" R package (Fuss, 2020; Hüppi et al., 2018). This package automatically selects the optimal model to describe changes in gas concentrations, thereby preventing artifacts from gas saturation in the headspace. Conversion from gas concentration to fluxes required chamber temperature and air pressure, both obtained from the nearby meteorological station.

2.3.3. Carbon and GHG balance

For the harvest export (C_{Export}), the carbon content was either measured (unpolished dry matter rice) or taken from the literature on ley (Bolinder et al., 2012; Ma Su Hui et al.,2018); carbon was assumed to return to the atmosphere upon consumption. The carbon balance is described from an atmospheric perspective, which gives GPP a negative sign, as it represents a loss of carbon from the atmosphere, whereas all other terms of the carbon balance are positive, representing a gain of carbon in the atmosphere:

$$C_{Balance} = NEE + CH_4 + C_{Export} \quad (4)$$

To obtain the annual budget for CH_4 and N_2O, linear interpolation was used to obtain daily fluxes for the days on which no measurements were carried out. The resulting continuous fluxes were summed to obtain annual budgets. The total annual budgets of the individual gases were multiplied by their 100-year global warming potential (GWP) (CH_4: 27; N_2O: 273; Smith et al., 2021) to express the annual budgets as CO_2-equivalent.

In the GHG balance, the harvest export was included:

$$GHG_{Balance} = GPP + R_{eco} + CH_4 \bullet GWP_{CH_4} + N_2O \bullet GWP_{N_2O} + CO_{2,Export} \quad (5)$$

2.4. Statistics

For the statistical analysis, R software (version 4.4.3) was used. First, the residuals of the GHG budgets were checked for normality by visual inspection with a qq-plot and the Shapiro–Wilk test with the help of the olsrr package. For non-normal cases, the GHG budgets were transformed logarithmically to achieve a normal distribution of the residuals. Second, the residuals were tested for homoscedasticity using a Breusch–Pagan test from the car package. A one-way ANOVA was then used to test whether the treatments had significantly different annual GHG budgets ($p < 0.05$). As this was the case, the Tukey post hoc test was used to assess the difference between the three individual treatments. The difference was seen as significant if the p-value was < 0.05. Effect size was calculated with standardized mean difference (Cohen's d). Sensitivity analyses based on the measurement uncertainty of the devices were conducted. Numbers are provided together with their standard deviation in parenthesis. Test statistics and residual plots are listed in the supplementary material (Table S2-S5, Figure S6-7).

3. Results

3.1. CO_2 exchange

The R_{eco}–temperature relationship revealed an exponential dependency for both drained and flooded conditions. Flooding had a clearly decreasing effect on R_{eco}, especially at temperatures below 20°C (Fig. 1).

Cumulative NEE was significantly higher in DL compared to FR and FR+AC ($p < 0.001$, Cohen's d > 1.77), but there was no significant difference between FR and FR+AC ($p = 0.2$, Cohen's d = 1.09) (Table 1). At the start of measurements before seedling transplantation in May 2023, all mesocosms had a positive NEE, indicating a higher R_{eco} than GPP (Fig. 2a). As the season progressed, cumulative NEE became negative in FR and FR+AC as GPP outweighed R_{eco}, whereas the cumulative NEE of the DL increased throughout the entire experiment. The difference in cumulative NEE was strongest at the harvest drainage at the end of the rice season when the cumulative NEE of FR was −4.5 t CO_2 ha^{-1}, in FR+AC −5.0 t CO_2 ha^{-1}, and 18.8 t CO_2 ha^{-1} in DL

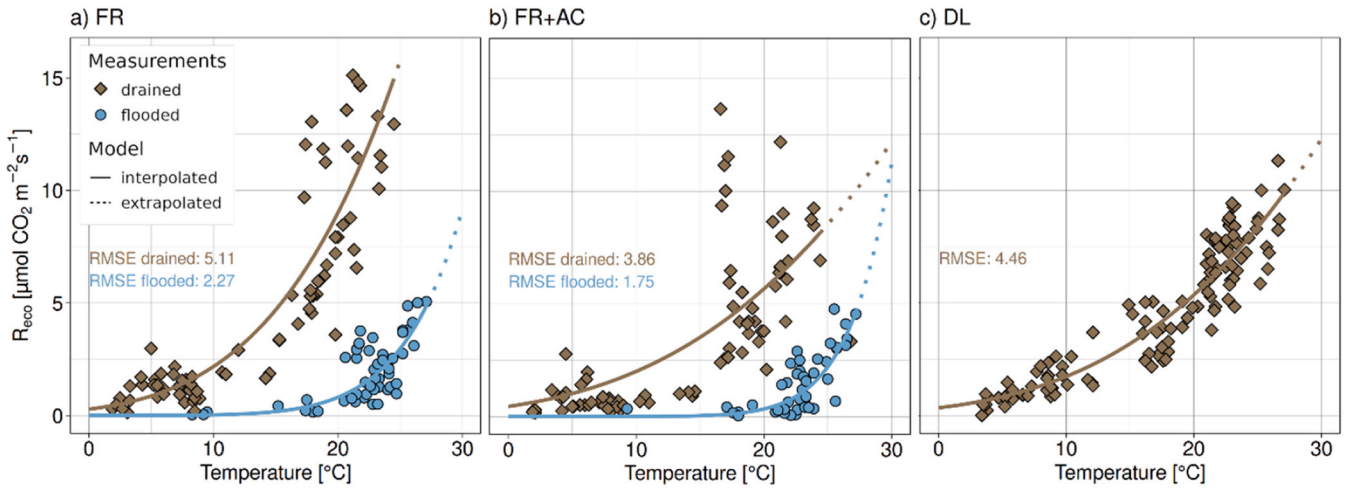

Fig. 1. Ecosystem respiration (R_{eco}) related to temperature. (a) flooded rice (FR), (b) flooded rice with amended mineral cover (FR+AC), (c) drained ley (DL) with root mean squared error (RMSE). The points denote all measurements taken throughout one year. The solid line shows the Arrhenius model fitted to the measurement points (Eq. 2), and the dotted part represents where extrapolation was necessary. Brown diamonds are measurement values conducted under drained conditions, while blue points were measured during flooded conditions.

Table 1
Mean and standard deviation of annual GHG fluxes and balances of GHG and carbon (including carbon exported in harvest) in mesocosms with flooded rice (FR), flooded rice with amended mineral cover (FR+AC), and drained ley (DL) cultivation (4 replicates). NEE stands for net ecosystem exchange (NEE = GPP + R_{eco}), GPP for gross primary production, and R_{eco} for ecosystem respiration. Positive numbers indicate net emissions to the atmosphere.

	Unit	FR	FR+AC	DL
NEE	t CO_2 ha^{-1} yr^{-1}	8.5 (2.2)	3.3 (5.5)	24.2 (3.5)
GPP	t CO_2 ha^{-1} yr^{-1}	-22.7 (1.7)	-21.0 (3.1)	-25.9 (1.7)
R_{eco}	t CO_2 ha^{-1} yr^{-1}	31.3 (1.9)	24.3 (7.1)	50.1 (4.0)
Harvest export	t C ha^{-1} yr^{-1}	2.9 (0.3)	2.5 (0.4)	1.7 (0.7)
CH_4	kg CH_4 ha^{-1} yr^{-1}	54.3 (26.6)	40.2 (15.2)	-1.1 (0.2)
	t CO2-eq. ha^{-1} yr^{-1}	1.5 (0.7)	1.1 (0.4)	-0.03 (0.005)
N_2O	kg N_2O-N ha^{-1} yr^{-1}	0.9 (0.4)	0.7 (0.5)	5.6 (4.2)
	t CO2-eq. ha^{-1} yr^{-1}	0.2 (0.1)	0.2 (0.1)	1.5 (1.1)
GHG balance	t CO2-eq. ha^{-1} yr^{-1}	20.9 (2.7)	14.0 (6.3)	32.7 (7.0)
C balance	t C ha^{-1} yr^{-1}	5.3 (0.7)	3.5 (1.7)	8.4 (1.6)

(Fig. 2a).

A day before mid-season drainage, the NEE was negative −0.5 (0.03) g CO_2 m^{-2} h^{-1} in FR and −0.4 (0.05) g CO_2 m^{-2} h^{-1} in FR+AC (Figure S8). The lowering of the water table for the mid-season drainage in August turned NEE positive (0.8 (0.3) g CO_2 m^{-2} h^{-1} in FR and 0.4 (0.2) g CO_2 m^{-2} h^{-1} in FR+AC). The reason for the positive NEE rates was the high R_{eco} following drainage. The summed R_{eco} during the mid-season drainage accounted for 8.8 % of the annual R_{eco} of the FR plots and 7.7 % of that of the FR+AC plots. Following reflooding 9 days later, NEE values were comparable to those before the mid-season drainage (FR: −0.5 (0.1) g CO_2 m^{-2} h^{-1}, FR+AC: −0.4 (0.2) g CO_2 m^{-2} h^{-1}) (Figure S8).

Following the final drainage for harvest in September, NEE in FR and FR+AC rose again from negative to positive values, resulting in the highest NEE measured all year (Figure S8). The summed R_{eco} over the six days following the drainage accounted for 7.8 % of the total annual R_{eco} in FR and for 6.7 % in FR+AC. During winter, all mesocosms remained drained, and daily NEE was consistently positive (Figure S8). At the end of the measurement period of a full crop cycle in April 2024, all mesocosms had a positive cumulative NEE, with the exception of one of the FR+AC mesocosms (Fig. 2b). R_{eco} during drained conditions accounted for 61.6 % of the annual total R_{eco} in FR and 68.4 % in FR+AC. Analysis of the R_{eco} models for a hypothetical off-season flooding (end of September to seedling transplantation mid-May) to assess potential GHG balance improvements revealed that R_{eco} was reduced by 40 % in FR over the whole year.

3.2. CH_4 emissions

Cumulative CH_4 emissions were higher in FR and FR+AC compared to DL, with DL acting as a minor CH_4 sink (Table 1). Although mean total CH_4 emissions were lower in FR+AC compared to FR, this difference was not significant ($p = 0.77$, Cohen's d = 0.66) (Fig. 3b). CH_4 fluxes correlated non-linearly and negatively with redox potential in FR and FR+AC ($p < 0.001$) (Figure S9).

In May 2023, when the mesocosms were freshly flooded, CH_4 fluxes were very low. After 4 weeks of flooding, CH_4 fluxes began to rise in FR and FR+AC (Fig. 3a). CH_4 fluxes increased during July and were high before mid-season drainage in August (FR: 3.8 (1.6 mg) CH_4 m^{-2} h^{-1}, FR+AC: 2.2 (0.4) mg CH_4 m^{-2} h^{-1}) (Figure S10). Mid-season drainage in August reduced CH_4 emissions in nearly all mesocosms by 68 % in FR and 85 % in FR+AC. Following reflooding after this drainage event, CH_4 fluxes increased slower than before the drainage. The final drainage for harvest caused a pulse of CH_4 emissions accounting for 5.2 (2.6)% of the annual CH_4 emission (FR: 6.3 (3.8) mg CH_4 m^{-2} h^{-1}, FR+AC: 5.1 ± 3.4 mg CH_4 m^{-2} h^{-1}) (Fig. 3a). These were the highest CH_4 fluxes recorded during the entire measurement period. Thereafter, all mesocosms were drained during winter, resulting in very low or negative CH_4 fluxes during this period (Figure S10). CH_4 fluxes in DL were negative throughout the entire measurement period.

3.3. N_2O emissions

FR had 83.9 % lower cumulative N_2O emission compared to DL ($p = 0.025$, Cohen's d = 1.26) (Fig. 4b). The difference between FR and FR+AC was not significant ($p = 0.61$, Cohen's d = 0.36) (Table 1). N_2O emissions were strongly related to fertilization events (Fig. 4a). N_2O peaks following fertilization were responsible for 89.3 % of total N_2O emissions in all treatments. After the second fertilization event in mid-June, N_2O emissions increased strongly in the DL plots (DL: 0.9 (1.4) mg N_2O-N m^{-2} h^{-1}) (Figure S11). This second fertilization event

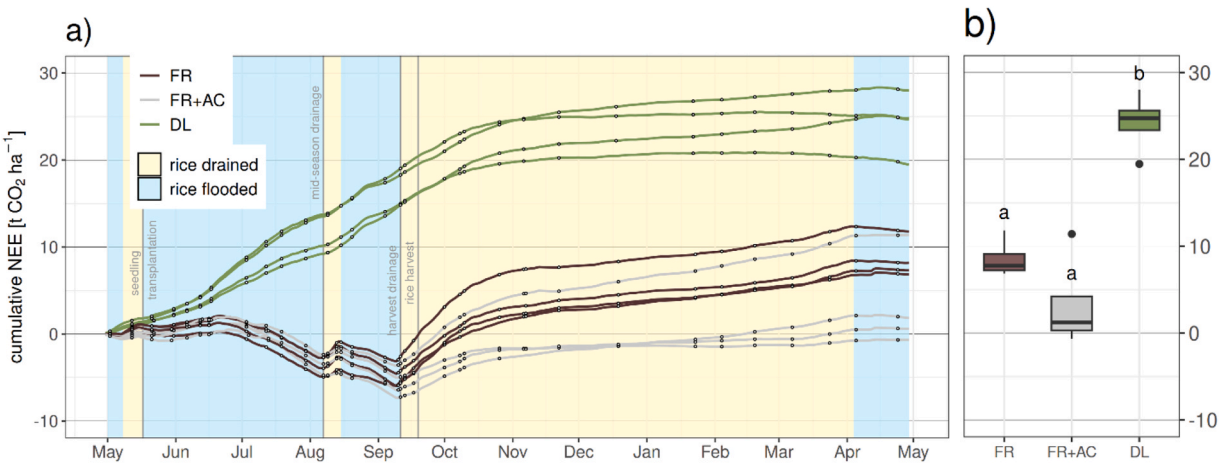

Fig. 2. a) Modeled cumulative net ecosystem exchange (NEE) of CO_2 of flooded rice (FR), flooded rice with amended mineral cover (FR+AC), and drained ley (DL) over one year (May 2023-May 2024). The beige background denotes periods when rice mesocosms were drained and light blue when rice mesocosms were flooded. The black points along the lines mark the measurement time points. b) Boxplot of cumulative annual NEE.

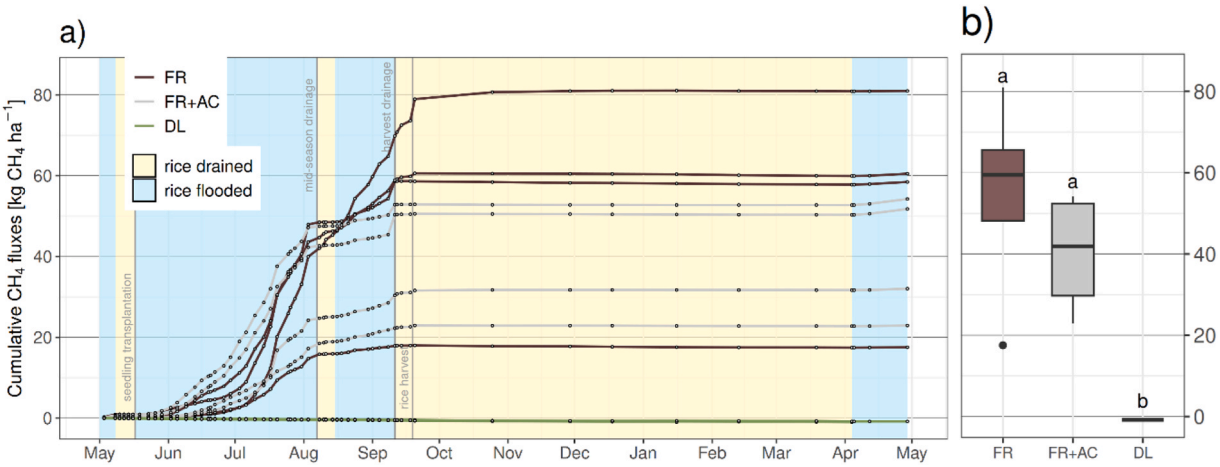

Fig. 3. a) Cumulative annual CH_4 fluxes of flooded rice (FR), flooded rice with amended mineral cover (FR+AC), and drained ley (DL) over the whole measurement period of one year (May 2023-May 2024). The beige background denotes periods when rice mesocosms were drained and light blue when rice mesocosms were flooded. The black points along the lines mark the measurement time points. b) Boxplot of cumulative annual CH_4 fluxes.

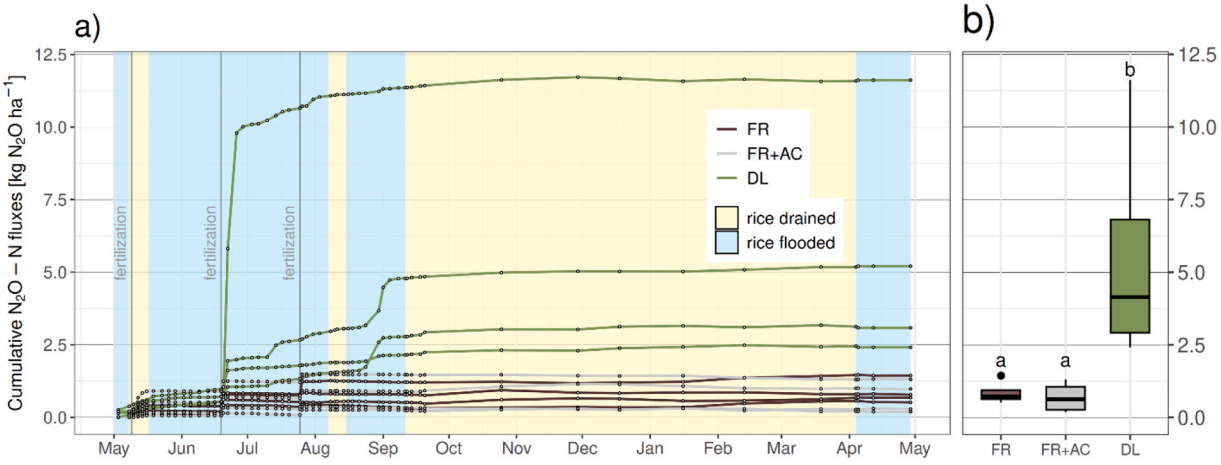

Fig. 4. a) Cumulative annual N_2O emissions of flooded rice (FR), flooded rice with amended mineral cover (FR+AC), and drained ley (DL) over the whole measurement period of one year (May 2023–May 2024). The beige background denotes periods when rice mesocosms were drained, and the light blue background shows when rice mesocosms were flooded. The black points along the lines mark the measurement time points. b) Boxplot of cumulative annual N_2O fluxes.

coincided with rainfall of 28.3 mm over 4 days and had a ratio of N_2O-N: total fertilizer N applied of 0.05. At the end of August, after heavy precipitation of 76.6 mm over 3 days following prolonged dry conditions (Figure S12), another N_2O emission burst occurred in DL with no associated fertilizer event (0.3 (0.3) mg N_2O-N m^{-2} h^{-1}, ratio of N_2O-N: total fertilizer N applied: 0.03). Over the whole measurement period the ratio of N_2O-N:total fertilizer N applied was 0.15 in DL. In FR and FR+AC, N_2O emissions increased only during the third fertilization event at the end of July. N_2O emissions were unaffected by drainage events in FR and FR+AC. In the off-season months from mid-September 2023 to April 2024, N_2O emissions were low in all mesocosms, accounting for 1.4 (1.1)% of the annual N_2O emissions in DL and 22.6 (18.8)% in FR, and negative in FR+AC. In FR the ratio of N_2O-N:total fertilizer N applied over the whole year was 0.008 and 0.006 in FR+AC.

3.4. Carbon and GHG balance

All treatments had a positive carbon balance acting as a carbon source. Differences in carbon balance between treatments were primarily induced by R_{eco} (Table 1). FR and FR+AC had significantly lower R_{eco} compared to R_{eco} in DL ($p < 0.001$). Although total R_{eco} was lower in FR+AC compared to FR, the reduction was not significantly different from FR ($p = 0.15$). For GPP, only the difference between DL and FR+AC was significant ($p = 0.02$). CH_4 emissions had a negligible share of the total carbon balance of all treatments. The C_{export} was significantly lower in DL compared to FR and FR+AC ($p < 0.02$).

In summary, over the course of one year, the net GHG balance was highest in DL (Table 1). FR had a 36.1 % lower net GHG balance compared to DL ($p = 0.03$, Cohen's d = 1.47), and FR+AC showed an even greater decrease by 57.2 % ($p = 0.004$, Cohen's d = 1.59) using the 100-year global warming potential of each gas according to Eq. 5. The difference between FR and FR+AC was not significant ($p = 0.37$, Cohen's d = 1.19). The GHG balance was dominated by CO_2 emissions in all treatments, accounting for 91 % in FR and FR+AC and 95 % in DL (Fig. 5). CH_4 only accounted for 8 % of the total GHG balance in the paddy rice treatments, while N_2O emissions accounted for 1 %. In DL, CH_4 emissions were negative, and N_2O emissions were responsible for 5 % of the GHG balance.

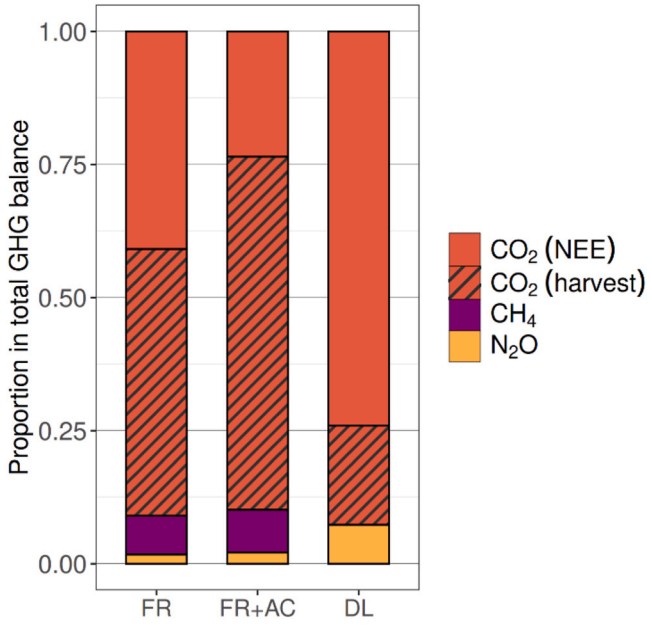

Fig. 5. Share of each GHG on the total GHG balance in flooded rice (FR), flooded rice + amended mineral cover (FR+AC), and drained ley (DL). Net ecosystem exchange (NEE) is the sum of gross primary production (GPP) and ecosystem respiration (R_{eco}). CO_2 (harvest) represents the carbon in the exported biomass converted to CO_2.

4. Discussion

4.1. Paddy rice cultivation can reduce the net GHG balance of managed organic soil

In this experiment, paddy rice cultivation significantly reduced the net GHG balance relative to the currently drained use of organic soils (Table 1). This improvement was mostly due to reduced CO_2 emissions under flooded conditions compared to the DL treatment (Fig. 2b). Although high water tables during the rice season also led to an increase in CH_4 emissions (Fig. 3b), a beneficial net effect of flooding prevailed, given that the saved CO_2 more than compensated for the emitted CH_4 (Fig. 5). Rewetting organic soils not only reduces CO_2 emissions but also mitigates N_2O emissions (Tiemeyer et al., 2016). Indeed, rice treatments emitted less than one fifth of N_2O emissions compared to DL (Fig. 4). Overall, the induced CH_4 emissions associated with paddy rice cultivation were strongly outweighed by the reduced CO_2 and N_2O emissions.

Given that this experiment was conducted in a mesocosm setup, it is important to know whether the DL treatment, serving as a reference, accurately reflects the typical GHG values of cool temperate grassland on drained organic soil. The carbon balance obtained in this study is almost equal to that of Tiemeyer et al. (2020). N_2O emissions in DL were also within the range of other studies on drained organic soil in the cool temperate climate (Koch et al., 2023; Tiemeyer et al., 2020). Overall, the GHG measurements from DL show that this outdoor mesocosm setup produced comparable results and that drained ley treatment was a suitable reference for cool temperate grassland on deeply drained organic soils.

4.2. Drivers of individual budget components

Although the higher water table in the flooded rice treatments could not completely stop peat decomposition, it strongly reduced CO_2 emissions (Fig. 1). Lowering the water table, however, caused high CO_2 emissions peaks. For example, during mid-season drainage, R_{eco} strongly increased (Fig. 2a). This CO_2 emission peak was attributed to degassing following the reduction of hydrostatic pressure and increased oxygen availability, resulting in higher R_{eco} values (Haque et al., 2016; Knox et al., 2015). This has also been observed in warm temperate rice fields with organic soil, which reported a similar CO_2 emission peak during mid-season drainage, with a similar share in total annual R_{eco} (Hatala et al., 2012; Knox et al., 2015). However, both studies reported an annual R_{eco} that was one third higher compared to this study, although their fields were, in contrast to this experiment, flooded in winter. Among other reasons, these higher R_{eco} values might be due to higher temperatures in warm temperate climate. Temperature is a major driver of R_{eco} (Fig. 1).

CH_4 emissions in this experiment were equal (Naser et al., 2007) or half as high (Nishimura et al., 2020) as those measured in a mineral paddy field in cool temperate northern climate. However, CH_4 emissions in this study were unexpectedly low, given that organic soils under paddy rice cultivation emit about two times more CH_4 than mineral soils (Kajiura et al., 2018). An explanation for the low CH_4 emissions potentially lies in the multiple water table adjustments made during the season. Although CH_4 emission rates usually increase over the rice season (Hatala et al., 2012; Nishimura et al., 2020), this was observed to a limited extent in this study (Figure S10). A possible reason for this difference could be the short drainage events of several hours used for fertilization (Figure S5). This was apparently enough time to increase the redox potential above −180 mV, which is generally considered the threshold below which methanogenesis occurs (Yu et al., 2001). Additionally, the low CH_4 emissions recorded in this study might be because straw was not returned to the site prior to the experiment. The addition of straw is known to increase CH_4 emissions in paddy rice cultivation

(Conrad, 2002; Kajiura et al., 2018).

Compared to the N_2O emissions measured in this experiment, studies from mineral paddy fields in cool temperate northern Japan reported slightly lower N_2O emissions (Naser et al., 2019; Nishimura et al., 2020). This discrepancy is mostly linked to less N fertilizer application. Despite the DL treatment receiving less fertilizer than FR and FR+AC, its N_2O emissions were higher in DL. One possible explanation is that N_2O emissions in drained organic soils mainly stem from soilborne N rather than from N applied by fertilization (Wang et al., 2024). Furthermore, the prolonged water-saturated conditions during the rice season (May-September 2023) resulted in a strong reduction of redox potential (Figure S5), establishing anaerobic conditions. This most likely led to complete denitrification with N_2 instead of N_2O as an end-product as it is often the case in continuously flooded rice paddies (Peyron et al., 2016; Zhou et al., 2017). However, the N-cycle was not quantified in this study and without NH_4^+ and NO_3^- pore water measurements the low N_2O emissions in rice mesocosms cannot be clearly linked to complete denitrification, which is a limitation of this study. Furthermore, it is impossible to say to which degree the differing N-fertilizer input between DL and the rice treatments affected N_2O emissions

4.3. Effect of amended mineral cover on GHG emissions

The amended mineral cover had a reducing effect on CO_2 emissions, but this was not significant. Similarly, Paul et al. (2024) did not find a decrease in CO_2 emissions due to mineral cover under field conditions. Although CH_4 emissions were reduced by amended mineral cover, this effect was not significant, in line with the findings by Wüst-Galley et al. (2023) for the same experimental site. Based on previous work, also it was expected that mineral cover would reduce N_2O emissions (Paul et al., 2024; Wang et al., 2022; Wüst-Galley et al., 2023), but this was not found. Differences in the water table and soil aeration are the most plausible factors for these diverging results. Whereas the mineral cover was aerobic in Wang et al. (2022) and Wüst-Galley et al. (2023), the water table in this study was several centimeters above the soil surface, possibly resulting in complete denitrification following the low redox potential (Peyron et al., 2016; Zhou et al., 2017).

Compost addition was necessary to biologically activate the nutrient-poor subsoil used as cover in 2020 as it is common agricultural practice. It cannot be excluded that this affected the GHG balance. Prior work has shown that organic amendments like compost may (Jeong et al., 2018; Yagi and Minami, 1990) or may not increase CH_4 emissions from rice fields (Yan et al., 2005). Furthermore, compost application reduces bulk density and increases porosity (Kranz et al., 2020) and therefore affects gas diffusion during drainage events, which can be responsible for peaks in CO_2 and CH_4 emissions (Han et al., 2005; Hatala et al., 2012). Overall, the reducing effect on GHG emissions of the mineral cover alone might have been more pronounced without compost application, but this experimental setup does not allow to quantify that.

4.4. Comparison of paddy rice on organic soil with paludiculture

One motivation for this study was to evaluate paddy rice as an additional option to paludiculture for managing organic soils under a high water table. Thus, the question remains how the GHG balance of paddy rice cultivation on organic soils compares to the GHG balance of common paludiculture crops. The CO_2-related terms (including harvest) in this experiment were in the range of values of studies on several paludiculture crops in Europe reviewed by Bianchi et al. (2021), although the rice mesocosms were drained over winter. Non-sphagnum paludiculture crops in Bianchi et al. (2021) emitted 4.5 times more CH_4 most likely because they had an all-year-round higher water table compared to the FR mesocosms. Similarly, Tiemeyer et al. (2020) reported a fivefold higher CH_4 emissions in rewetted organic soils compared to the FR treatment of this study. The CH_4 emissions recorded in FR were similar to those from paludiculture crops with water levels below the surface (Günther et al., 2015), presumably because the water table in the rice mesocosms was above the soil surface only from May to September. As for N_2O in paludiculture, emissions fall below the detection limit (Günther et al., 2015; Minke et al., 2016) or tend to be of a similarly low magnitude, as measured in the FR mesocosms (Bianchi et al., 2021; Tiemeyer et al., 2020). Together, the total GHG balance across different paludiculture crops was, on average, 18 t CO_2 eq ha^{-1} yr^{-1} in Europe (Bianchi et al., 2021). The reported value is very close to this study's GHG balance (20.9 t CO_2 eq ha^{-1} yr^{-1}) and indicates that paddy rice on organic soil could be as beneficial as a paludiculture crop in terms of its GHG mitigation potential. While economic feasibility of rice as a local niche product is clearly given (Fabian et al., 2024) other practical constraints to large-scale implementations such as water availability, weed pressure, and policy barriers need to be addressed in future studies.

4.5. Management option for further reducing the GHG balance of paddy rice on organic soil

All rice mesocosms were drained during off-season (September 2023–April 2024), which is in line with farmer's practice in Switzerland. During this time, 62 % of R_{eco} occurred in FR. Therefore, off-season flooding in rice cultivation could further reduce the net GHG balance in this experiment. To test this possibility, the R_{eco} model obtained for flooded conditions was used to simulate off-season flooding. The result indicates that total R_{eco} could be further reduced by about 40 % in FR. Since N_2O emissions were mostly linked to fertilization and were minimal during flooded conditions, it can be assumed that they would be negligible during off-season flooding without fertilization. However, the overall improvement in off-season flooding for the GHG balance cannot be precisely determined, as flooding would probably increase CH_4 emissions. Knox et al. (2016) found CH_4 emissions of 65.3 kg CH_4 ha^{-1} under flooded conditions during off-season months. This accounted for 44 % of their annual CH_4 emissions. If the reported relationship of off-season to annual CH_4 emissions was applied to this experiment, it would result in off-season CH_4 emissions of 23.8 kg CH_4 ha^{-1}. Overall, winter flooding as an alternative form of management would then lead to a total annual GHG balance of 9.5 t CO_2-eq ha^{-1} yr^{-1}, which is a hypothetical reduction of approximately 55 % compared to the current GHG balance in FR and would be 71 % better than the GHG balance in DL (Table 1). Clearly, this is only a rough estimate of how the CH_4 emission would develop under off-season flooding but paired with the results from this study's R_{eco} model, it suggests that the effect would be beneficial for the GHG balance. Apart from this management option, future research on reducing the net GHG balance further could focus on CH_4-mitigating straw management such as turning it into biochar (Han et al., 2016; Nan et al., 2020) or composting it (Launio et al., 2016).

4.6. Study limitations

While the results of this study indicate that paddy rice cultivation on organic soils could reduce net GHG emissions compared to ley on drained organic soil, it is also important to discuss the limitations on the scope of this study. First, this study was conducted over the course of a year and, therefore, cannot account for interannual variability of the system. Weather conditions can strongly influence the carbon balance. For example, Knox et al. (2016) observed a paddy rice field on organic soil in California to be a carbon sink in a colder year, whereas it turned into a carbon source in a hot year. Exported biomass C from DL was less than half compared to a relatable study (Paul et al., 2024) due to a heatwave in June and August, which resulted in a partial dieback of ley despite additional watering. This strongly affects the DL GHG balance, possibly resulting in a lower GHG balance due to reduced C export. On the other hand, high temperatures result in CO_2 emission peaks (Figure S8 and S12), which would lead to a higher GHG balance. Furthermore, peaks in N_2O emissions after intense rainfall following a

dry period were observed, highlighting the importance of weather conditions for GHG measurements. Second, conducting GHG measurements on mesocosm-scale might not yield the same results as measurements on field-scale due to edge effects and temperature differences (Teuben and Verhoef, 1992). Therefore, a multi-annual GHG balance on field-scale is necessary to generalize this study's results.

5. Conclusion

This study assessed the net GHG balance of an innovative solution to a long-standing problem in cool temperate Europe, namely the negative impact of drained farmed peatlands on soils and climate. To date, the necessary rewetting associated with paludiculture has only been taken up on a small scale due to the lack of markets, that is, economic feasibility, and impacts on food security. Growing paddy rice as a new crop in the cool temperate climate offers an alternative that is currently economically attractive as a local niche product for farmers in Switzerland. For the first time in Europe north of the Alps, all relevant GHGs were measured for paddy rice cultivation on organic soil. The results show a potential in the reduction of the net GHG balance with paddy rice cultivation by more than one third compared to traditional drained management of organic soil, despite higher CH_4 emissions with its higher global warming potential, and similar GHG benefits as other paludiculture crops. Furthermore, additional reduction in the net GHG balance of this cultivation system could be possible by off-season flooding. While the results of this study are promising, it could not account for interannual variability nor was it conducted under field-scale conditions. Therefore, this study justifies further research on multi-annual field scale into GHG mitigation options for rice cultivation on organic soils in the cool temperate zone.

CRediT authorship contribution statement

Lisa Tamagni: Writing – review & editing, Investigation, Data curation. **Alina Widmer:** Writing – review & editing, Writing – original draft, Visualization, Methodology, Investigation, Formal analysis, Data curation. **Sonja Paul:** Writing – review & editing, Supervision, Project administration, Conceptualization. **Chloé Wüst-Galley:** Writing – review & editing, Visualization, Supervision, Project administration, Investigation, Formal analysis, Data curation, Conceptualization. **Markus Jocher:** Software, Methodology, Investigation. **Sebastian Doetterl:** Writing – review & editing, Supervision. **Valerio Volpe:** Methodology, Investigation, Data curation. **Jens Leifeld:** Writing – review & editing, Supervision, Funding acquisition, Conceptualization. **Thomas Keller:** Writing – review & editing, Supervision.

Declaration of Generative AI and AI-assisted technologies in the writing process

During the preparation of this work the author(s) used Copilot in order to improve the readability of the text and ensure that the text is written consistently in American English. After using this tool/service, the author(s) reviewed and edited the content as needed and take full responsibility for the content of the published article.

Declaration of Competing Interest

The authors declare that they have no known competing financial interests or personal relationships that could have appeared to influence the work reported in this paper.

Acknowledgements

Many thanks to Robin Giger, Fabio Elvedi, Regina Widmer, Maria Vorkauf, Johannes Koestel, and Juliane Hirte (Agroscope, Switzerland) who assisted in the measurements. Furthermore, we extend our gratitude to Kevin Kramer, Amelie Kreuzer, Marcio Martins, Marco Ketzel, and Cyrill Zosso (Agroscope, Switzerland) for rice seedling transplantation and harvest. Special thanks go to Matthias Volk (Agroscope, Switzerland) for his advice on CO_2 measurements and data analysis. Research funding for this study was partly provided by the Swiss National Science Foundation (Switzerland, grant number: 40B2-0_203536).

Appendix A. Supporting information

Supplementary data associated with this article can be found in the online version at doi:10.1016/j.agee.2025.110146.

Data availability

The cumulative flux data (CO2, CH4, N2O) are available at Zenodo (DOI: 10.5281/zenodo.15367139)

References

Bianchi, A., Larmola, T., Kekkonen, H., Saarnio, S., Lång, K., 2021. Review of greenhouse gas emissions from rewetted agricultural soils. Wetlands 41, 1–7.

Bickel, K., Richards, G., Köhl, M., & Rodrigues, R.L. (2006). Consistent representation of lands. In H.S. Eggleston, L. Buendia, K. Miwa, T. Ngara, & K. Tanabe (Eds.), 2006 IPCC guidelines for national greenhouse gas inventories: Volume 4 Agriculture, forestry and other land use (pp. 3.1–3.42). IPCC.

Bolinder, M.A., Kätterer, T., Andren, O., Parent, L.E., 2012. Estimating carbon inputs to soil in forage-based crop rotations and modeling the effects on soil carbon dynamics in a Swedish long-term field experiment. Can. J. Soil Sci. 92 (6), 821–833.

Buschmann, C., Röder, N., Berglund, K., Berglund, Ö., Lærke, P.E., Maddison, M., Mander, Ü., Myllys, M., Osterburg, B., van den Akker, J.J.H., 2020. Perspectives on agriculturally used drained peat soils: comparison of the socioeconomic and ecological business environments of six European regions. Land Use Policy 90, 104181. https://doi.org/10.1016/j.landusepol.2019.104181.

Conrad, R., 2002. Control of microbial methane production in wetland rice fields. Nutr. Cycl. Agroecosyst. 64, 59–69.

Crush, J.R., Nichols, S.N., Easton, H.S., Ouyang, L., Hume, D.E., 2009. Comparisons between wild populations and bred perennial ryegrasses for root growth and root/shoot partitioning. N. Z. J. Agric. Res. 52 (2), 161–169.

DIN, 2022. DIN EN 15936:2022-09 Soil, waste, treated biowaste and sludge - Determination of total organic carbon (TOC) by dry combustion. 10.31030/3293536.

Drösler, M. (2005). Trace Gas Exchange and Climatic Relevance of Bog Ecosystems, Southern Germany [Doctoral dissertation, Technische Universität München].

Erkens, G., Van der Meulen, M.J., Middelkoop, H., 2016. Double trouble: subsidence and CO2 respiration due to 1,000 years of Dutch coastal peatlands cultivation. Hydrogeol. J. 24 (3), 551.

Evans, C.D, Peacock, M, Baird, A.J, Artz, R.R.E, Burden, A, Callaghan, N, Chapman, P.J, Cooper, H.M, Coyle, M, Craig, E, Cumming, A, Dixon, S, Gauci, V, Grayson, R.P, Helfter, C, Heppell, C.M., Holden, J., Jones, D.L., Kaduk, J., Levy, P., Matthews, R., McNamara, N.P., Misselbrook, T., Oakley, S., Page, S.E., Rayment, M., Ridley, L.M., Stanley, K.M., Williamson, J.L., Worrall, F., Morrison, R., 2021. Overriding water table control on managed peatland greenhouse gas emissions. Nature 593 (7860), 548–552. https://doi.org/10.1038/s41586-021-03523-1.

Fabian, Y., Hutchings, C., Wüst-Galley, C., Jacot, K., Walder, F., Holzkämpfer, A., 2024. Alternative landwirtschaftliche Kulturen auf Feuchtackerflächen im Umfeld von Mooren in der Schweiz. Agrosc. Sci. *190*. https://doi.org/10.34776/as190g.

Fabian, Y., Roberti, G., Jacot, K., Gramlich, A., Benz, R., Szerencsits, E., Churko, G., Prasuhn, V., Leifeld, J., Zorn, A., Walter, T., Herzog, F., 2022. Die Nutzung von vernässenden Ackerflächen neu denken: synthese des Projektes "Feucht (Acker) Flächen. Agrar. Schweiz 13, 198–209. https://doi.org/10.34776/afs13–198 g.

Ferré, M., Muller, A., Leifeld, J., Bader, C., Müller, M., Engel, S., Wichmann, S., 2019. Sustainable management of cultivated peatlands in Switzerland: insights, challenges, and opportunities. Land Use Policy 87, 104019.

Freeman, B.W., Evans, C.D., Musarika, S., Morrison, R., Newman, T.R., Page, S.E., Jones, D.L., 2022. Responsible agriculture must adapt to the wetland character of mid-latitude peatlands. Glob. Change Biol. 28 (12), 3795–3811.

Fuss, R., 2020. Gasfluxes: greenhouse gas flux calculation from chamber measurements. R. Package Version 0, 4, 4.

Günther, A., Huth, V., Jurasinski, G., Glatzel, S., 2015. The effect of biomass harvesting on greenhouse gas emissions from a rewetted temperate fen. GCB Bioenergy 7 (5), 1092–1106.

Han, X., Sun, X., Wang, C., Wu, M., Dong, D., Zhong, T., Thies, J., Wu, W., 2016. Mitigating methane emission from paddy soil with rice-straw biochar amendment under projected climate change. Sci. Rep. 6 (1), 24731.

Han, G.H., Yoshikoshi, H., Nagai, H., Yamada, T., Saito, M., Miyata, A., Harazono, Y., 2005. Concentration and carbon isotope profile of CH4 in paddy rice canopy: isotopic evidence for changes in CH4 emission pathways upon drainage. Chem. Geol. 218, 25–40.

Haque, M.M., Kim, G.W., Kim, P.J., Kim, S.Y., 2016. Comparison of net global warming potential between continuous flooding and midseason drainage in monsoon region paddy during rice cropping. Field Crops Res. 193, 133–142.
Hatala, J.A., Detto, M., Sonnentag, O., Deverel, S.J., Verfaillie, J., Baldocchi, D.D., 2012. Greenhouse gas (CO2, CH4, H2O) fluxes from drained and flooded agricultural peatlands in the Sacramento-San Joaquin Delta. Agric. Ecosyst. Environ. 150, 1–18.
Huguenin-Elie, O., Mosimann, E., Schlegel, P., Luescher, A., Kessler, W., & Jeangros, B. (2017) Düngung von Grasland in Grundlagen für die Düngung landwirtschaftlicher Kulturen in der Schweiz (GRUD). Agroscope.
Hüppi, R., Felber, R., Krauss, M., Six, J., Leifeld, J., Fuß, R., 2018. Restricting the nonlinearity parameter in soil greenhouse gas flux calculation for more reliable flux estimates. PloS One 13 (7), e0200876.
IUSS Working Group W.R.B. (2022). World Reference Base for Soil Resources. International soil classification system for naming soils and creating legends for soil maps. 4th edition. International Union of Soil Sciences (IUSS), Vienna, Austria.
Jeong, S.T., Kim, G.W., Hwang, H.Y., Kim, P.J., Kim, S.Y., 2018. Beneficial effect of compost utilization on reducing greenhouse gas emissions in a rice cultivation system through the overall management chain. Sci. Total Environ. 613, 115–122.
Johnson, K.A., Goody, R.S., 2011. The original Michaelis constant: translation of the 1913 Michaelis–Menten paper. Biochemistry 50 (39), 8264–8269.
Joosten, H., Gaudig, G., Krawczynski, R., Tanneberger, F., Wichmann, S., Wichtmann, W., 2015. Managing soil carbon in Europe: Paludicultures as a new perspective for peatlands. Soil carbon: Science, management and policy for multiple benefits. CABI, pp. 297–306.
Jurasinski, G., Koebsch, F., Guenther, A., Beetz, S., & Jurasinski, M.G. (2014). Package 'flux'. Flux rate calculation from dynamic closed chamber measurement: R.
Kajiura, M., Minamikawa, K., Tokida, T., Shirato, Y., Wagai, R., 2018. Methane and nitrous oxide emissions from paddy fields in Japan: an assessment of controlling factor using an intensive regional data set. Agric. Ecosyst. Environ. 252, 51–60.
Knox, S.H., Matthes, J.H., Sturtevant, C., Oikawa, P.Y., Verfaillie, J., Baldocchi, D., 2016. Biophysical controls on interannual variability in ecosystem-scale CO2 and CH4 exchange in a California rice paddy. J. Geophys. Res. Biogeosci. 121 (3), 978–1001.
Knox, S.H., Sturtevant, C., Matthes, J.H., Koteen, L., Verfaillie, J., Baldocchi, D., 2015. Agricultural peatland restoration: effects of land-use change on greenhouse gas (CO2 and CH4) fluxes in the Sacramento-San Joaquin Delta. Glob. Change Biol. 21 (2), 750–765.
Koch, J., Elsgaard, L., Greve, M.H., Gyldenkærne, S., Hermansen, C., Levin, G., Shubiao, W., Stisen, S., 2023. Water table driven greenhouse gas emission estimate guides peatland restoration at national scale. Biogeosci. Discuss. 2023, 1–28.
Kraehmer, H., Thomas, C., Vidotto, F., 2017. Rice production in Europe. In: Chauhan, B., Jabran, K., Mahajan, G. (Eds.), Rice production worldwide. Springer. https://doi.org/10.1007/978-3-319-47516-5_4.
Kranz, C.N., McLaughlin, R.A., Johnson, A., Miller, G., Heitman, J.L., 2020. The effects of compost incorporation on soil physical properties in urban soils–a concise review. J. Environ. Manag. 261, 110209.
Launio, C.C., Asis, C.A., Manalili, R.G., Javier, E.F., 2016. Cost-effectiveness analysis of farmers' rice straw management practices considering CH4 and N2O emissions. J. Environ. Manag. 183, 245–252.
Leifeld, J., Menichetti, L., 2018. The underappreciated potential of peatlands in global climate change mitigation strategies. Nat. Commun. 9 (1), 1071.
Leifeld, J., Müller, M., Fuhrer, J., 2011. Peatland subsidence and carbon loss from drained temperate fens. Soil Use Manag. 27 (2), 170–176.
Leifeld, J., Wüst-Galley, C., Page, S., 2019. Intact and managed peatland soils as a source and sink of GHGs from 1850 to 2100. Nat. Clim. Change 9, 945–947. https://doi.org/10.1038/s41558-019-0615-5.
Lim, J.Y., Cho, S.R., Kim, G.W., Kim, P.J., Jeong, S.T., 2021. Uncertainty of methane emissions coming from the physical volume of plant biomass inside the closed chamber was negligible during the cropping period. Plos One 16 (9), e0256796.
Linquist, B., Van Groenigen, K.J., Adviento-Borbe, M.A., Pittelkow, C., Van Kessel, C., 2012. An agronomic assessment of greenhouse gas emissions from major cereal crops. Glob. Change Biol. 18 (1), 194–209.
Liu, Y., Ge, T., Zhu, Z., Liu, S., Luo, Y., Li, Y., Wang, P., Gavrichkova, O., Xu, X., Wang, J., Wu, J., Guggenberger, G., Kuzyakov, Y., 2019. Carbon input and allocation by rice into paddy soils: a review. Soil Biol. Biochem. 133, 97–107.
Lloyd, J., Taylor, J.A., 1994. On the temperature dependence of soil respiration. Funct. Ecol. 8, 315–323.
Ma Su Hui, M.S., He Feng, H.F., Tian Di, T.D., Zou Dong Ting, Z.D., Yan Zheng Bing, Y.Z., Yang Yu Long, Y.Y., Fang Jing Yun, F.J., 2018. Variations and determinants of carbon content in plants: a global synthesis. Biogeosciences 15, 693–702.
Maier, M., Weber, T.K., Fiedler, J., Fuss, R., Glatzel, S., Huth, V., Jordan, S., Jurasinski, G., Kutzbach, L., Schaefer, K., Weymann, D., Hagemann, U., 2022. Introduction of a guideline for measurements of greenhouse gas fluxes from soils using non-steady-state chambers. J. Plant Nutr. Soil Sci. 185 (4), 447–461.
Minke, M., Augustin, J., Burlo, A., Yarmashuk, T., Chuvashova, H., Thiele, A., Freibauer, A., Tikhonov, V., Hoffmann, M., 2016. Water level, vegetation composition, and plant productivity explain greenhouse gas fluxes in temperate cutover fens after inundation. Biogeosciences 13, 3945–3970. https://doi.org/10.5194/bg-13-3945-2016.
Nan, Q., Yi, Q., Zhang, L., Ping, F., Thies, J.E., Wu, W., 2020. Biochar amendment pyrolysed with rice straw increases rice production and mitigates methane emission over successive three years. Waste Manag. 118, 1–8.
Naser, H.M., Nagata, O., Sultana, S., Hatano, R., 2019. Carbon sequestration and contribution of CO2, CH4 and N2O fluxes to global warming potential from paddy-fallow fields on mineral soil beneath peat in Central Hokkaido. Jpn. Agric. 10 (1), 6.
Naser, H.M., Nagata, O., Tamura, S., Hatano, R., 2007. Methane emissions from five paddy fields with different amounts of rice straw application in central Hokkaido, Japan. Soil Sci. Plant Nutr. 53 (1), 95–101.
Nishimura, S., Kimiwada, K., Yagioka, A., Hayashi, S., Oka, N., 2020. Effect of intermittent drainage in reduction of methane emission from paddy soils in Hokkaido, northern Japan. Soil Sci. Plant Nutr. 66 (2), 360–368.
Oestmann, J., Tiemeyer, B., Düvel, D., Grobe, A., Dettmann, U., 2022. Greenhouse gas balance of Sphagnum farming on highly decomposed peat at former peat extraction sites. Ecosystems 25 (2), 350–371.
Paul, S., Ammann, C., Wang, Y., Alewell, C., Leifeld, J., 2024. Can mineral soil coverage be a suitable option to mitigate greenhouse gas emissions from agriculturally managed peatlands? Agric. Ecosyst. Environ. 375, 109197.
Peyron, M., Bertora, C., Pelissetti, S., Said-Pullicino, D., Celi, L., Miniotti, E., Romani, M., Sacco, D., 2016. Greenhouse gas emissions as affected by different water management practices in temperate rice paddies. Agric. Ecosyst. Environ. 232, 17–28.
Rawlins, A., Morris, J., 2010. Social and economic aspects of peatland management in Northern Europe, with particular reference to the English case. Geoderma 154 (3-4), 242–251.
Reiser, R., Stadelmann, V., Weisskopf, P., Grahm, L., Keller, T., 2020. System for quasi-continuous simultaneous measurement of oxygen diffusion rate and redox potential in soil. J. Plant Nutr. Soil Sci. 183 (3), 316–326.
Richardson, A.D., Braswell, B.H., Hollinger, D.Y., Burman, P., Davidson, E.A., Evans, R. S., Flanagan, L.B., Munger, J.W., Savage, K., Urbanski, S.P., Wofsy, S.C., 2006. Comparing simple respiration models for eddy flux and dynamic chamber data. Agric. For. Meteorol. 141 (2-4), 219–234.
Saunois, M., Martinez, A., Poulter, B., Zhang, Z., Raymond, P., Regnier, P., Canadell, J.G., Jackson, R.B., Patra, P.K., Bousquet, P., Ciais, P., Dlugokencky, E.J., Lan, X., Allen, G.H., Bastviken, D., Beerling, D.J., Belikov, D.A., Blake, D.R., Castaldi, S., Zhuang, Q., 2024. Global methane budget 2000–2020. Earth Syst. Sci. Data Discuss. https://doi.org/10.5194/essd-2024-115.
Smith, C., Nicholls, Z.R.J., Armor, K., Collins, W., Forster, P., Meinshausen, M., Palmer, M.D., Watanabe, M., 2021. The earth's energy budget, climate feedbacks, and climate sensitivity Suppl.ary material. In: Masson-Delmotte, V., Zhai, P., Pirani, A., Connors, S.L., P'ean, C., Berger, S., Caud, N., Chen, Y., Goldfarb, L., Gomis, M.I., Huang, M., Leitzell, M., Lonnoy, E., Matthews, J.B.R., Maycock, T.K., Waterfield, T., Yelekçi, O., Yu, R., Zhou, B. (Eds.), Climate Change. The physical science basis. Contribution of Working Group I to the Sixth assessment report of the Intergovernmental Panel on Climate Change 9. Cambridge University Press, pp. 1–2391. https://doi.org/10.1017/9781009157896.
Sriskandarajah, N., Wüst-Galley, C., Heller, S., Leifeld, J., Määttä, T., Ouyang, Z., Malhotra, A., 2024. Sci. Rep. 14 (1), 14593.
Su, P., Zhang, A., Wang, R., Wang, J.A., Gao, Y., Liu, F., 2021. Prediction of future natural suitable areas for rice under representative concentration pathways (RCPs). Sustainability 13 (3), 1580.
Tanneberger, F., Appulo, L., Ewert, S., Lakner, S., Ó Brolcháin, N., Peters, J., Wichtmann, W., 2021b. The power of nature-based solutions: how peatlands can help us to achieve key EU sustainability objectives. Adv. Sustain. Syst. 5 (1), 2000146.
Tanneberger, F., Birr, F., Couwenberg, J., Kaiser, M., Luthardt, V., Nerger, M., Birr, F., 2022. Saving soil carbon, greenhouse gas emissions, biodiversity and the economy: paludiculture as sustainable land use option in German fen peatlands. Reg. Environ. Change 22, 69.
Tanneberger, F., Moen, A., Barthelmes, A., Lewis, E., Miles, L., Sirin, A., Tegetmeyer, C., Joosten, H., 2021a. Mires in Europe—Regional diversity, condition and protection. Diversity 13 (8), 381. https://doi.org/10.3390/d13080381.
Teuben, A., Verhoef, H.A., 1992. Relevance of micro-and mesocosm experiments for studying soil ecosystem processes. Soil Biol. Biochem. 24 (11), 1179–1183.
Tiemeyer, B., Albiac Borraz, E., Augustin, J., Bechtold, M., Beetz, S., Beyer, C., Drösler, M., Eickenscheidt, T., Ebli, M., Fiedler, S., Förster, C., Freibauer, A., Giebels, M., Glatzel, S., Heinichen, J., Hoffmann, M., Höper, H., Jurasinski, G., Leiber-Sauheitl, K., Zeitz, J., 2016. High emissions of greenhouse gases from grasslands on peat and other organic soils. Glob. Change Biol. 22, 4134–4149. https://doi.org/10.1111/gcb.13303.
Tiemeyer, B., Freibauer, A., Borraz, E.A., Augustin, J., Bechtold, M., Beetz, S., Beyer, C., Ebli, M., Eickenscheidt, T., Fiedler, S., Forster, C., Gensior, A., Giebels, M., Glatzel, S., Heinichen, J., Hoffmann, M., Hoper, H., Jurasinski, G., Laggner, A., Leiber-Sauheitl, K., Peichl-Brak, M., Drösler, M., 2020. A new methodology for organic soils in national greenhouse gas inventories: data synthesis, derivation and application. Ecol. Indic. 109, 105838. https://doi.org/10.1016/j.ecolind.2019.105838.
United Nations Environment Programme (UNEP). (2022). Global Peatlands Assessment: the State of the World's Peatlands - Evidence for Action toward the Conservation, Restoration, and Sustainable Management of Peatlands. ⟨https://wedocs.unep.org/20.500.11822/41222⟩.
Volk, M., Obrist, D., Novak, K., Giger, R., Bassin, S., Fuhrer, J., 2011. Subalpine grassland carbon dioxide fluxes indicate substantial carbon losses under increased nitrogen deposition, but not at elevated ozone concentration. Global Change Biology 17 (1), 366–376.
Wang, Y., Calanca, P., Leifeld, J., 2024. Sources of nitrous oxide emissions from agriculturally managed peatlands. Glob. Change Biol. 30 (1), e17144.
Wang, Y., Paul, S.M., Jocher, M., Alewell, C., Leifeld, J., 2022. Reduced nitrous oxide emissions from drained temperate agricultural peatland after coverage with mineral soil. Front. Environ. Sci. 10, 856599.

Wüst-Galley, C., Heller, S., Ammann, C., Paul, S., Doetterl, S., Leifeld, J., 2023. Methane and nitrous oxide emissions from rice grown on organic soils in the temperate zone. Agric. Ecosyst. Environ. 356, 108641.
Yagi, K., Minami, K., 1990. Effect of organic matter application on methane emission from some Japanese paddy fields. Soil Sci. Plant Nutr. 36 (4), 599–610.
Yan, X., Yagi, K., Akiyama, H., Akimoto, H., 2005. Statistical analysis of the major variables controlling methane emission from rice fields. Glob. Change Biol. 11 (7), 1131–1141.
Yu, K., Wang, Z., Vermoesen, A., Patrick Jr, W., Van Cleemput, O., 2001. Nitrous oxide and methane emissions from different soil suspensions: effect of soil redox status. Biol. Fertil. Soils 34, 25–30.
Zhou, W., Xia, L., Yan, X., 2017. Vertical distribution of denitrification end-products in paddy soils. Sci. Total Environ. 576, 462–471.